

841 (K 6048

1986.837

Studies in Surface Science and Catalysis 24

# ZEOLITES

## Synthesis, Structure, Technology and Application

Proceedings of an International Symposium  
organized by the "Boris Kidrič" Institute of Chemistry, Ljubljana  
on behalf of the International Zeolite Association,  
Portorož-Portorose, September 3-8, 1984

Editors

**B. Držaj, S. Hočevar and S. Pejovnik**

*»Boris Kidrič« Institute of Chemistry, 61000 Ljubljana, Yugoslavia*



ELSEVIER

Amsterdam - Oxford - New York - Tokyo

1985

## CONTENTS

Studies in Surface Science and Catalysis .....	XI
Preface .....	XIII

## SYNTHESIS

Synthesis of zeolites (R.M. Barrer) (Plenary lecture) .....	1
The synthesis, crystallization and structure of heteroatom containing ZSM-5 type zeolite (M-ZSM-5) (Xu Ruren and Pang Wenqin (Plenary lecture).....	27
Synthesis of ZSM-5 type zeolites in the system $(\text{Na}, \text{K})_2\text{O}-\text{Al}_2\text{O}_3-\text{SiO}_2-\text{H}_2\text{O}$ without and with TPA Br (A. Nastro, C. Colella and R. Aiello) ....	39
Crystallization of ZSM-5 type zeolites from reaction mixtures free of organic cations (J.M. Berak and R. Mostowicz) .....	47
Nature and structure of high silica zeolites synthesized in presence of (poly) alkyl mono- and diamines (Z. Gabelica, M. Cavez-Bierman, P. Bodart, A. Gourgue, and J.B. Nagy) .....	55
Factors influencing the crystal morphology of ZSM-5 type zeolites (R. Mostowicz and J.M. Berak) .....	65
The influence of alkali metal cations on the formation of silicalite in $\text{NH}_4\text{OH}-\text{TBAOH}$ systems (Tu Kungang and Xu Ruren) .....	73
Template variation in the synthesis of zeolite ZSM-5 (F.J. van der Gaag, J.C. Jansen and H.van Bekkum) .....	81
The synthesis of high silica zeolites in the absence of sodium ion (Li Hongyuan, Liang Juan, Ying Muliang and Lin Baoxiang) .....	89
Synthesis of silica-high zeolites in the presence of surfactants (J. Batista, B. Držaj and A. Zajc) .....	97
Synthesis of offretite-erionite type zeolite from solution phase (S. Ueda, M. Nishimura, and M. Koizumi) .....	105
Studies on the transformation between erionite and offretite in T-type zeolite (Wang Xingqiao and Xu Ruren) .....	111
Synthesis and characterization of faujasite-type zeolites II. The role of alkali chlorides (N. Dewaele, P. Bodart, Z. Gabelica and J.B. Nagy) .....	119
A contribution to the synthesis of the low-silica X zeolite (M. Tatič and B. Držaj) .....	129

## VI

Optimization of faujasite synthesis using factorial design technique (M.K. Tannous, M. Helmy, F.H. Khalil and M.F. Abadir) .....	137
Synthesis of A, X and Y zeolites from clay minerals (E.B. Drag, A. Miecznikowski, F. Abo-Lemon, M. Rutkowski) .....	147
Synthesis of zeolite A and P from natural and waste materials (Ch. Stamboliev, N. Sopova, K.-H. Bergk and M. Porsch) .....	155
On the reaction mechanism of the formation of molecular sieves and related compounds (E. Wieker and B. Fahlke) (Plenary lecture) .....	161
A model for the computation of the species concentrations in aqueous silicate and aluminosilicate solutions (J.-L. Guth, P. Caullet and R. Wey) .....	183
The mechanism of transformation of NaY to NaPc type zeolites (Ma Shujie, Li Liansheng, Xu Ruren and Yie Zhaohui) .....	191
Kinetic analysis of autocatalytic nucleation during crystallization of zeolites (B. Subotić and A. Graovac) .....	199
Analysis of particulate processes during the transformation of Zeolite A into hydroxysodalite (B. Subotić, N. Mašić and I. Šmit) .....	207

## STRUCTURE DETERMINATION

Zeolite structures: Some common misconceptions and pitfalls (W.M. Meier) (Plenary lecture-extended abstract) .....	217
Characterization of zeolite catalysts by MAS NMR (G.T. Kokotailo, C.A. Fyfe, G.C. Gobbi, G.J. Kennedy, C.T. Deschutter, R.S. Ozubko and W.J. Murphy) (Plenary lecture) .....	219
The impact of new diffraction techniques in zeolite structural chemistry (J.M. Newsam and D.E.W. Vaughan) .....	239
Neutron diffraction studies of the hydrogen bonding and water molecules in zeolites (G.H. Artioli, J.V. Smith, Å.Kvick, J.J. Pluth and K. Ståhl) .....	249
On the influence of (Si, Al) disorder on the T-O distances measured in zeolites (A. Alberti and G. Gottardi) .....	255
Dealumination of Zeolites by volatile reagents. Mechanism of and structural changes caused by dealumination (P. Fejes, I. Kiricsi, I. Hannus and Gy. Schöbel) .....	263

Crystal structures of related novel aluminophosphate frameworks: AlPO <sub>4</sub> -21 (py), AlPO <sub>4</sub> -EN3 (en) and a structural model for AlPO <sub>4</sub> -25 (J.B. Parise) .....	271
IR study of framework vibrations and surface properties of high silica zeolites (Guo Wengui, Liang Juan, Li Hongyuan, Ying Muliang and Hu Jiehan) .....	279
<sup>13</sup> C nuclear magnetic resonance study of molecules adsorbed on ZSM-5 and silicalite (W. Meiler and H. Pfeifer) .....	287
Theoretical and experimental studies on the sorption of gases in silicalite (A.T.J. Hope, C.R.A. Catlow, C.A. Leng and C.J. Adams) .....	297
Silylation of H-ZSM-5. A TGA study (R. Von Ballmoos and G.T. Kerr) ...	307
Surface properties of phosphorus and magnesium modified ZSM-5 zeolites (Cai Guangyu, Chen Guoquan, Wang Qingxia, Xin Quin, Wang Xiangzhen, Wang Zuozhou, Li Xiyiao and Liang Juan) .....	319
Pore size engineering in zeolites (E.F. Vansant, G. Peeters, A. Thijs and I. Verhaert) .....	329
Thermal stability of mordenites with various SiO <sub>2</sub> /Al <sub>2</sub> O <sub>3</sub> ratios (I. Tsolovski, Chr. Minchev, E.E. Senderov and V. Penchev) .....	337
The thermodesorption kinetics of water from mordenite (V. Dondur and R. Dimitrijević) .....	345
Spectroscopy of Cu (II) coordinated to lattice oxygens in zeolites (D. Packet, W. Dehertogh and R.A. Schoonheydt) .....	351
Structural and thermal properties of exchanged forms of clinoptilolite from Zlatokop (Vranje), Yugoslavia (T. Čeranić, D. Vučinić, B. Držaj and S. Hočevar) .....	359
Study of the properties of clinoptilolite modified by transition metal ions (A. Spojakina, I. Tsolovski, N. Kostova, T. Popov, S. Krustev and D. Shopov) .....	367
Cuban natural zeolites: Morphological studies by electron microscopy (G.R. Fuentes, C.L. Sanchez, J.C. Romero and K.R. Malherbe) .....	375
Effect of the dealumination of Y-type zeolites on their wetting properties (I. Dékány, F. Szántó and H.K. Beyer) .....	385
Hydrothermal behaviour of Zeolites in FCC catalysts (I. Halász, J. Horváth, T. Mándy, L. Schmidt and E. Tasnády) .....	393

## VIII

Hydrothermal ageing of cracking catalysts. I. - Evaluation of the crystalline fraction of zeolites (F. Mauge, J.C. Courcelle, Ph. Engelhard, P. Gallezot, J. Grossmangin, M. Primet and B. Trusson)...	401
Matrix effects on the $M(CO)_2 + CO \rightleftharpoons M(CO)_3$ equilibrium experienced by monovalent rhodium and iridium carbonyls in zeolites (F. Lefebvre, A. Auroux and Y. Ben Taarit) .....	411
Preparation of iron(0) model catalysts with iron clusters of sub-nm dimensions by decomposition of Y-zeolite adsorbed iron pentacarbonyl (Th. Bein, F. Schmidt and P.A. Jacobs) .....	419
Gas chromatographic sorption studies of hydrocarbons in N-A-type zeolites with different Si/Al-ratios (H. Lechert and W. Schweitzer).	427
The $Cu^{2+}$ ion migration in the CuNaX zeolite (Wei Guoxiang, Ye Hujuan, Lü Guanglie, Liu Zhengyi, Song Deyu and Lin Bingxiong) .....	435
New method of determining the volume of adsorbent micropores (A.A. Fomkin, I.I. Seliverstova and V.V. Serpinsky).....	443
Crystal structure and mechanism of $Ag^+$ exchange on NaA.NaNO <sub>3</sub> inclusion complex of zeolite A (R. Dimitrijević, N. Petranović, I. Krstanović, M. Šušić and U. Mioč).....	453
Resolution of $\alpha$ - and $\beta$ -cage decapsulation peaks in the temperature programmed diffusion (TPD) of non-polar gases in Cs, Na-A (D. Fraenkel, B. Ittah and M. Levy) .....	459
Ordered distribution of cations in zeolite A (T. Takaishi, T. Ohgushi and K. Nonaka) .....	467
Heat capacities of water in zeolites (V. Vučelić and D. Vučelić) .....	475
Gismondine: The detailed X-ray structure refinement of two natural samples (R. Rinaldi and G. Vezzalini) .....	481
Factors affecting acidity and basal spacing of cross-linked smectites (Liu Zhonghui and Sun Guida) .....	493

## TECHNOLOGY AND APPLICATION

Natural zeolites: Processing, present and possible applications (R. Sersale) (Plenary lecture).....	503
Chemical <sup>Behandlung</sup> treatment of natural zeolites, and properties and utilizations of the reacted materials (H. Minato) .....	513

Natural zeolites as constituents of blended cements (R. Sersale and G. Frigione) .....	523	
Use of clinoptilolite in paper industry as filler of paper (Zhang Quanchang, Su Minqdi, Dai Changlu, Yang Huarui, Zhang Qixing and Zhang Zhiguo) .....	531	
Ammonia removal from municipal water by phillipsite (P. Ciambelli, P. Corbo, L. Liberti, A. Lopez and C. Porcelli) .....	539	
X Application of natural zeolites in refrigeration (S.L. Zhukoborsky)..	547	X
X Energy storage in zeolites and application to heating and air conditioning (D. Jung, N. Khelifa, E. Lavemann and R. Sizmann) .....	555	X
The release of tritiated water from zeolites into surrounding water (M. Todorović, I. J. Gal and I. Paligorić) .....	563	✓
Sodiumtriphosphate replacement by builder systems in detergents (L. Gabrovšek) .....	571	
Synthesis of zeolite A from silicate raw materials and its application in formulations of detergents (S. Donevska, J. Tanevski and N. Daskalova) .....	579	+
Some rheological and transport properties of zeolite suspensions (V. Grilc and B. Držaj) .....	585	✓
Zeolites NaHA and CaHA as toothpaste abrasives (E.P. Hertenberg and A.L. Dent) .....	589	
Pressure swing adsorption on 4A and 5A zeolite (N.S. Raghavan, M.M. Hassan and D.M. Ruthven) .....	597	
X Zeolites as adsorbents for alcohols from aqueous solutions (G.S. Haegh) .....	605	X
High silica zeolite as heterogeneous catalyst (Liang Juan) (Plenary lecture) .....	611	
Zeolite Nu-3: Its synthesis, characterisation and use in methanol conversion (J.L. Casci and T.V. Whittam) .....	623	
Catalytic properties of ZSM-11 and ZSM-5 zeolites (G. Giannetto, G. Perot and M. Guisnet) .....	631	
Initiating effect of $C_2^+$ olefins and alcohols on the transformations of methanol on crystalline and amorphous aluminosilicates (S. Dzwigaj, J. Haber and M. Derewinski) .....	639	

X

IR study of the cis-trans isomerization of olefins on H-ZSM-5 zeolite (C.P. Bezouhanova, C. Dimitrov, E. Khalilov and H. Lechert) .....	647
✓ The possibility of zeolite application in the used motor oil refining process (N. Jovanović, D. Skala, M. Marjanović, M. Stanković and T. Zerarka) .....	653
Nickel and/or molybdenum containing zeolites as catalysts for hydrodesulfurization (N. Davidova, P. Kovacheva and D. Shopov) .....	659
✓ Transalkylation of toluene with trimethyl benzenes over nickel supported type L-zeolite catalyst (A.B. Halgeri and T.S.R. Prasada Rao) .....	667
Kinetics of n-hexane isomerization on Pt/La-faujasite catalysts (M. Kh. Tannous, Ch. Marcilly and F.M. Khalil) .....	675
Low aromatic solvents through dearomatization on molecular sieve 13 X (D. Ahmetović and S. Švel - Čerovečki) .....	683

*Handwritten signature or mark*

## PREPARATION OF IRON(0) MODEL CATALYSTS WITH IRON CLUSTERS OF SUB-NM DIMENSIONS BY DECOMPOSITION OF Y-ZEOLITE ADSORBED IRON PENTACARBONYL

Th. BEIN<sup>1</sup>, F. SCHMIDT<sup>1</sup> and P.A. JACOBS<sup>2</sup>

<sup>1</sup>Institut für Physikalische Chemie der Universität Hamburg, Laufgraben 24,  
D-2000 Hamburg 13 (F.R.G.)

<sup>2</sup>Laboratorium voor Oppervlaktescheikunde, Kardinaal Mercierlaan, 92,  
B-3030 Heverlee (Belgium)

### ABSTRACT

Thermal decomposition in a shallow bed of iron pentacarbonyl adsorbed on NaY-zeolite is achieved under vacuum already at 370 K with low heating rates. Decomposition under fast heating in inert gas and fluidized shallow bed conditions can be completed within a few minutes at ca. 500 K. Zeolite supported iron clusters obtained by these techniques are characterized via evaluation of the respective magnetic isotherms taken with a Foner magnetometer at 4.2 K. Low temperature/vacuum as well as high temperature/inert gas thermolysis gives iron cluster systems with at least 70 to 90 wt-% smaller than 1 nm.

### INTRODUCTION

Several efforts have been made in order to investigate particle size effects in catalysis<sup>1,2,3</sup>. In particular, iron systems used in ammonia synthesis<sup>4</sup> and CO-hydrogenation reactions<sup>5</sup> are of industrial interest.

Since zeolites are crystalline and have well defined pore structure, variable electronic<sup>6</sup> and solvolytic properties, they are suitable supports for model catalysts.

In attempt to overcome difficulties in the preparation of iron zeolites by classical reduction techniques such as decreased reducibility of iron exchanged samples or contamination of the metal phase using alkali metals as reductants, the decomposition of preadsorbed iron pentacarbonyl was studied in detail<sup>7</sup>. The aim of these investigations is to dispose of iron model catalysts with defined, narrow particle size distribution.

Adsorption equilibrium between  $\text{Fe}(\text{CO})_5$  and different large pore zeolites was studied by gravimetric and IR-spectroscopic techniques<sup>8,9</sup>, whereas thermal decomposition was followed by thermogravimetric and IR-spectroscopic<sup>10</sup> methods. The effect of preparation conditions on iron particle size<sup>11</sup> will be reported in the present study in greater detail. The influence of different heating rates in a fluidized shallow bed reactor on iron particle size was studied by magnetic methods.



## EXPERIMENTAL

### Materials

Synthetic NaY(FAU) with Si/Al = 2.46 from Strem Chemicals was treated with 0.1 M NaCl solution, washed, air-dried and stored over saturated  $\text{NH}_4\text{Cl}$  solution to ensure constant humidity. Before loading with  $\text{Fe}(\text{CO})_5$ , the zeolite was degassed in the reactor at 670 K for 36 ks at  $10^{-3}$  Pa, with a heating rate of  $0.033 \text{ K s}^{-1}$ . Iron pentacarbonyl from Ventron (99.5%) was coldly distilled in the dark and stored in a stainless steel tube over molecular sieve 5A.

### Gas dosing system and reactor

A stainless steel gas dosing system with metal/viton valves, connected to a quartz reactor, allowed<sup>7</sup> controlled degassing of the hydrated zeolites under high vacuum ( $10^{-3}$  Pa), loading of the zeolites with purified dry vapor of  $\text{Fe}(\text{CO})_5$ , thermal and photochemical decomposition of the adducts in a shallow fluidized bed and sample preparation in inert atmosphere for magnetic measurements and Mössbauer spectroscopy.

After cooling 180 - 450 mg of dehydrated zeolite in the quartz reactor with a 20 x 50 mm horizontal bed section, iron carbonyl was frozen in liquid air, degassed and allowed to warm up to 273 K, and finally contacted with the zeolite sample. An equilibrium pressure of 870 Pa saturated the zeolite pore system<sup>9</sup>. After 14 ks, the system was evacuated for one hour. Subsequently, the adducts were decomposed thermally under vacuum or in helium gas, using a very fast heating procedure ("shock" heating). The latter was achieved by dipping the frozen reactor into a metal bath at 490 K.

The fluidized bed was generated by a horizontal vibration of the reactor with  $\nu = 50$  Hz and about 1 mm amplitude.

### Magnetization measurements

About 20 mg of iron zeolite sample was pressed with a quartz rod into a quartz tube (2.5 mm diameter) under vacuum, sealed off and introduced into the helium cryostat (Janis) of a Foner vibrating sample magnetometer (P.A.R.).

The magnetization curve was taken at 4.2 K in magnetic fields up to 6 T.

The magnetometer was calibrated with a pure Ni metal sample and corrections for sample holder and quartz tube were taken into account.

Most samples did not show hysteresis. Therefore, to a first approximation, the evaluation of the magnetic isotherms was carried out in terms of superparamagnetism. This implies that the magnetic measuring time is sufficient for the attainment of spin equilibrium, particle anisotropy, particle interaction and chemically inhomogeneous phases can be neglected.

Under these assumptions, the numerical reconstruction of the magnetic isotherms by a sum of different Langevin-<sup>12</sup> or Brillouin-functions<sup>13</sup> gives appro-

ximated weight fractions of particles with different sizes or cluster spin quantum numbers,  $I$ , respectively.

The Brillouin function

$$B_I(x) = M/M_\infty = \frac{2I + 1}{2I} \coth \frac{2I + 1}{2I} x - \frac{1}{2I} \coth \frac{1}{2I} x ,$$

with  $x = I g \mu_B B / kT$  applies to particles with a small magnetic moment.

( $M$  = magnetization,  $M_\infty$  = saturation magnetization,  $I$  = cluster spin quantum number,  $g$  = Landé factor,  $\mu_B$  = Bohr's magneton,  $B$  = magnetic field,  $k$  = Boltzmann's constant,  $T$  = temperature)

In attempt to obtain the saturation magnetization  $M_\infty$ , the iron content of the samples was determined by X-ray fluorescence and neutron activation techniques. The total relative error in iron weight is  $\pm 15\%$ .

## RESULTS AND DISCUSSION

Different heating rates in the range between  $0.0025$  and about  $10 \text{ K s}^{-1}$  were used during thermolysis of carbonyl/FAU-adducts.

The sample to which the slowest heating rate was applied (FAU/0.0025), was treated in a static bed under vacuum, because very slow heating under inert gas conditions may give an inhomogeneously distributed iron phase.

All other samples were decomposed under fluidized bed conditions in helium atmosphere. The respective decomposition parameters are given in table 1. The rate and degree of decomposition can be monitored following the gas pressure.

TABLE 1. Thermolysis of  $\text{Fe}(\text{CO})_5$ /FAU-adducts under fluidized shallow bed conditions<sup>a</sup>

Sample	Heating rate/ $\text{K s}^{-1}$	Final Temp. $T_{\text{max}}/\text{K}$	Heating period at $T_{\text{max}}/\text{ks}$	Helium-pressure /kPa	Outgassing <sup>b</sup> ks	Iron content /wt-%	Amount <sup>c</sup> CO/%
F/0.0025 <sup>d</sup>	0.0025	373	18	$10^{-2}$ Pa	-	5.2	-
F/0.33	0.33	490	0.24	48	50	5.3	88
F/S	ca. 10	490	0.36	80	54	3.9	88

<sup>a</sup>These preparations were carried out with amounts of dry zeolite ranging from 185 to 444 mg.

<sup>b</sup>At 373 K and  $10^{-3}$  Pa.

<sup>c</sup>Amount of CO generated with respect to the theoretical amount expected for an initial loading of 30 wt-%  $\text{Fe}(\text{CO})_5$ .

<sup>d</sup>This sample was decomposed under static bed conditions.

Representative pressure curves obtained at decomposition rates of  $0.33 \text{ K s}^{-1}$

(sample F/0.33) and "shock" heating (sample F/S), respectively, are shown in fig. 1.

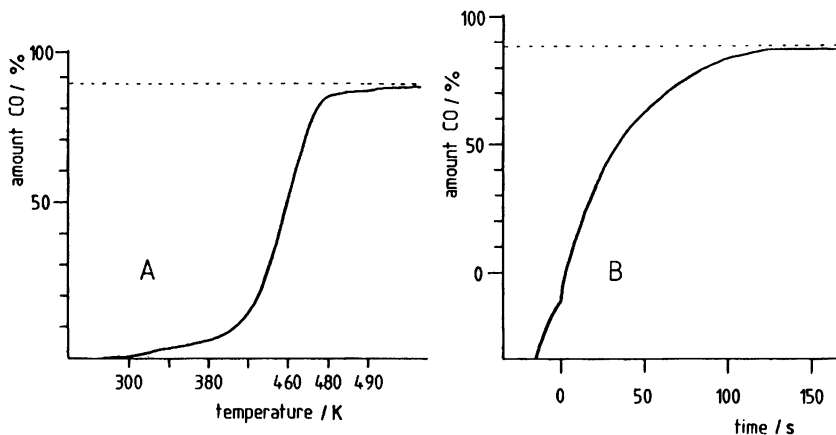


Fig. 1. Gas evolution curves during thermal decomposition of  $\text{Fe}(\text{CO})_5/\text{FAU}$ -adduct under fluidized bed conditions.

A, with a heating rate of  $0.33 \text{ K s}^{-1}$ , sample F/0.33;

B, with shock heating (sample F/S); parameters see table 1.

In the first case, the gas evolution rate clearly allows us to divide the decarbonylation process into three distinct regions: two zones of slow gas evolution are separated by a fast reaction (fig. 1a). The latter is accompanied by the typical color change from ivory-like to black.

Obviously, this curve resembles those obtained during thermogravimetric experiments with similar  $\text{Fe}(\text{CO})_5/\text{zeolite}$  adducts<sup>8,10</sup> and confirms independently the picture of a fast, endothermic reaction, splitting off the main carbonyl fraction to give relatively thermostable, highly unsaturated polynuclear carbonyl clusters.

If in contrast the adduct is heated by a temperature shock, the slow gas evolution prior to the main reaction is missing (fig. 1b).

Quantitative interpretation of these volumetric data shows that decarbonylation occurs in a reproducible and complete manner (table 1), irrespective of the heating rate and the amount of sample.

Characterization of the thermally decomposed samples was done via evalua-

tion of the respective magnetization curves at  $T = 4.2$  K. A representative curve (F/0.33) is depicted in fig. 2, whereas the results for other samples are given in table 2. As can be seen from table 2, in most cases one single

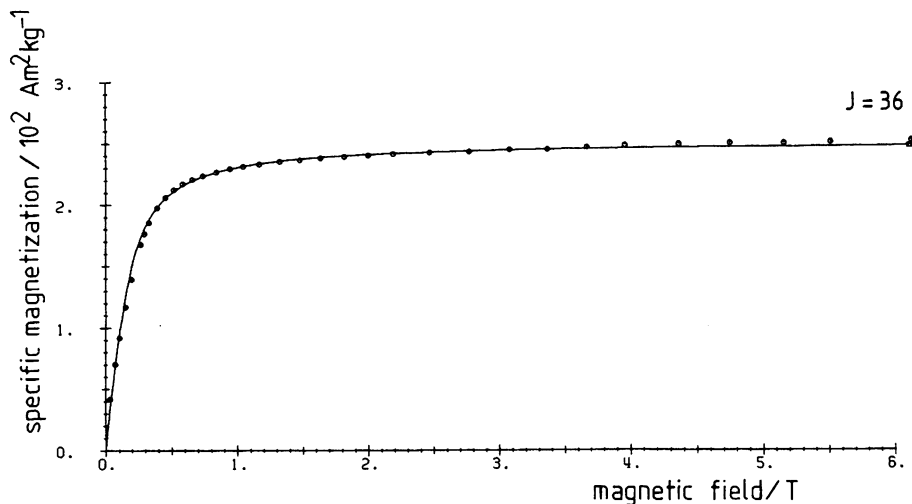


Fig. 2. Magnetization curve of sample F/0.33 at  $T = 4.2$  K, fitted by one Brillouin function with  $I = 36$ . Parameters see table 1 and 2.

Brillouin function suffices to fit the experimental magnetization curve. Under the assumptions mentioned in the experimental section, the results allow us to conclude the following:

- Thermolysis of  $\text{Fe}(\text{CO})_5/\text{FAU}$ -adducts gives iron particle systems with superparamagnetic behavior. In attempt to determine the mass fraction of the superparamagnetic particles, the experimental saturation magnetization  $M_{\infty, \text{exp}}$  was related to the bulk value ( $M_{\infty}(4.2 \text{ K}) = 1.752 \cdot 10^6 \text{ Am}^{-1}$ ). The superparamagnetic fraction  $q = M_{\infty, \text{exp}}/M_{\infty}$  is found to be 100%, within the error of the iron content, for all samples.
- The main fraction of the particle system shows magnetic moments corresponding to clusters with linear dimensions below 1 nm.
- The mean cluster size seems to be nearly independent of the heating rate applied to the fluidized shallow bed (samples F/0.17, F/0.33, F/S). It can be assumed that fast heating under inert gas prevents the samples effectively from sintering - even at the considerably high final temperatures which are

used to complete the decomposition.

- Iron cluster sizes obtained by very slow heating up to 373 K under vacuum (sample F/0.0025) are comparable to those of the inert gas/fast heating samples discussed above.
- Separate testing of the applied fit procedure provided estimated values for fractions of magnetically blocked particles, which still do not change significantly the sample's magnetization curve at  $T = 4.2$  K. At this temperature, the used magnetic particle size determination is insensitive to fractions of greater particles (i.e. greater than about 3 nm) below 20 wt-%. Since these particles contain more than  $10^6$  atoms, their total number should be negligible.

Additional characterization of the iron/zeolite systems was obtained in a recent Mössbauer spectroscopic study<sup>19</sup>. A typical bulk iron hyperfine splitting of comparable samples at room temperature indicates that spin equilibrium is not attained in the time domain of the Mössbauer effect ( $10^{-9}$  s).

TABLE 2. Cluster spin quantum number distribution of thermally decomposed  $\text{Fe}(\text{CO})_5/\text{FAU}$ -adducts, derived from Brillouin-fits.

Sample	$I^a$	Number of atoms <sup>b</sup> / N	particle size <sup>c</sup> $V^{1/3}/\text{nm}$	weight fraction <sup>e</sup> / %	q-value <sup>d</sup> / %
F/0.0025	35	35	0.74	100	107
F/0.33	36	36	0.75	100	111
F/S	43	43	0.80	100	117

<sup>a</sup>A Landé-factor  $g = 2.06$  was used in the argument of the Brillouin function<sup>14</sup>.

<sup>b</sup>The number of atoms equals  $I$ , since the value of  $I=1$  per atom was assumed.

<sup>c</sup>Particle size was calculated assuming bcc structure and atomic radius of iron to be  $R = 0.124$  nm, according to  $V^{1/3} = 0.227 \cdot N^{1/3}$  with  $N =$  number of atoms<sup>15</sup>.

<sup>d</sup>The q-value indicates the ratio between experimental saturation magnetization  $M_{\infty, \text{exp}}$  as derived from the Brillouin fit and the bulk value  $M_{\infty}(4.2 \text{ K}) = 1.752 \cdot 10^6 \text{ Am}^{-1}$ .

<sup>e</sup>Mass fraction of the respective discrete particle size fraction.

The presence of a certain amount of **larger** particles could be detected independently by X-ray diffraction methods. A weak, broad line was found with the d-value of the  $\alpha\text{-Fe } d_{110}$ -line. Linebroadening allowed us to estimate the mean particle size of this fraction to be  $\bar{d} = 30 \text{ nm} \pm 20 \text{ nm}$  - including Gauss- and Cauchy-line profile into the calculation. Transmission electron micrographs of comparable samples indicate that the **large** particles stick to the outer surface of the zeolite crystals<sup>16</sup>.

- The final iron content of the thermally decomposed  $\text{Fe}(\text{CO})_5/\text{FAU}$ -adducts is in the range between 3 and 6 wt-% of dry zeolite, indicating a total iron loss

of about 50% with respect to the original iron carbonyl loading (after degassing saturated adducts at  $T = 295$  K, an iron loading of ca. 9 wt-% remains on FAU<sup>8,9</sup>). This relatively high iron content exceeds by far those obtained on  $\gamma$ -Al<sub>2</sub>O<sub>3</sub><sup>17</sup> or graphite<sup>18</sup>.

#### CONCLUSION

The thermal decomposition of zeolite adsorbed iron pentacarbonyl was studied in a quartz reactor under fluidized shallow bed conditions.

Magnetic isotherms of the respective samples taken in a Foner magnetometer under inert conditions were evaluated using a Brillouin fit.

Thermal decomposition of the Fe(CO)<sub>5</sub>/FAU-adduct is achieved under vacuum already at 370 K with low heating rates, whereas decomposition under fast heating rates can be completed within a few minutes at ca. 500 K. Low temperature/vacuum as well as high temperature/inert gas thermolysis gives iron cluster systems with at least 70 - 90 wt-% smaller than 1 nm, indicating the effective prevention from sintering by heating under fluidized bed conditions.

Additional characterization of the generated iron zeolites by Mössbauer spectroscopy<sup>19</sup>, EXAFS and catalytic testing is under way.

#### ACKNOWLEDGEMENTS

Th. B. is indebted to the "Alfried Krupp von Bohlen und Halbach-Stiftung" for a grant. P.A. J. acknowledges a permanent research position as "Senior Research Associate" from N.F.W.O.-F.N.R.S. (Belgium). Financial support from the "Fonds der Chemischen Industrie" and the "Deutsche Forschungsgemeinschaft" (DFG) (F.R.G.) is gratefully acknowledged.

#### REFERENCES

- 1 J.H. Sinfelt, Adv. Catal. 23 (1973) 91.
- 2 M. Boudart, L.D. Ptak, J. Catal. 16 (1970) 90.
- 3 P.A. Jacobs in: Catalysis by Zeolites, B. Imelik, C. Naccache, Y. Ben Taarit, C. Vedrine, G. Coudurier and H. Praliand, eds., Elsevier, Amsterdam (1980) 293.
- 4 M. Boudart, H. Topsøe, J.A. Dumesic, in: The Physical Basis for Heterogeneous Catalysis, E. Drauglis, R.I. Jaffee, eds., Plenum, New York (1974) 337.

- 5 P.A. Jacobs, D. van Wouwe, *J. Mol. Catal.* 17 (1982) 145.
- 6 P.A. Jacobs, *Catal. Rev. - Sci. Eng.* 24 (1982) 415.
- 7 Th. Bein, Dissertation, University of Hamburg (1984).
- 8 Th. Bein, P.A. Jacobs, F. Schmidt, in: *Metal Microstructures in Zeolites*, P.A. Jacobs, N.I. Jaeger, P. Jiru and G. Schulz-Ekloff, eds., Elsevier, Amsterdam (1982) 111.
- 9 Th. Bein, P.A. Jacobs, *J.C.S. Faraday Trans. I*, 79 (1983) 1819.
- 10 Th. Bein, P.A. Jacobs, *J.C.S. Faraday Trans. I* (1984) in press.
- 11 F. Schmidt, Th. Bein, U. Ohlerich, P.A. Jacobs, *Sixth International Zeolite Conference*, Reno, U.S.A. (1983), Butterworth, in press.
- 12 W. Romanowski, *Z. anorg. allg. Chem.* 351 (1967) 180.
- 13 F. Schmidt, U. Stapel, H. Walther, *Ber. Bunsenges. Phys. Chem.* 88 (1984) 310.
- 14 D.M.S. Bagguley, *Proc. Roy. Soc. (London) A* 228 (1955) 549.
- 15 R. van Hardeveld, F. Hartog, *Surface Sci.* 15 (1969) 189.
- 16 Th. Bein, P.A. Jacobs, unpublished results.
- 17 A. Brenner, D.A. Hucul, *Inorg. Chem.* 18 (1979) 2836.
- 18 J. Phillips, B. Clausen, J.A. Dumesic, *J. Phys. Chem.* 84 (1980) 1814.
- 19 Th. Bein, G. Schmiester, F. Schmidt, W. GunBer, G. Kaindl, accepted for publication at "3rd International Symposium on Small Particles and Inorganic Clusters", Berlin, July 1984.